Wear, *127* (1988) 207 - 217

OPTICAL FLANK WEAR MONITORING OF CUTTING TOOLS BY IMAGE PROCESSING

J. U. JEON and S. W. KIM*

Department of Production Engineering, Korea Advanced Institute of Science and Technology, P. O. Box 150, Chongyang, Seoul (Korea)

(Received February 23, 1988; revised June 1, 1988; accepted June 8, 1988)

Summary

An optoelectronic method for *in situ* monitoring of the flank wear of cutting tools is presented. The method is based on real time vision technology in which the tool is illuminated by the beam of a laser and the wear zone is visualized using a Vidicon camera. The image is converted into digital pixel data and processed, to detect the wear land width. Detailed aspects of the image processing procedures are discussed along with the experimental results. As a conclusion, it has been proved that the average and maximum peak values of the flank wear width can be monitored effectively to a measuring resolution of 0.1 mm.

1. Introduction

The necessity for appropriate tool wear control becomes more important especially in modern machining systems in which many numerically controlled and computerized numerically controlled machines are operated in a more flexible and unmanned manner. For the control to be performed successfully, the *in situ* measurement of tool wear is of crucial importance in obtaining the necessary information for the tool during operation. For this purpose, several methods have been studied during the last few decades by many workers [1]. These methods may be classified into two groups: direct and indirect methods. The direct methods, as the name implies, are based upon direct measurements of the worn area on the tool using an optical sensor, television camera, pneumatic probe and so forth [2, 3]. These methods have the advantage of high measuring accuracy but cannot easily be adopted for *in situ* applications mainly because of the interruption of coolant and workpiece. Furthermore, no suitable and fast real time signal processing techniques have yet been developed. Various indirect methods have also been researched for many years in which the state of wear is estimated using calibration procedures which

*Author to whom correspondence should be addressed.

0043-1648/88/$3.50

involve measuring process parameters which have particular relationships with tool wear. Examples of such process parameters are cutting force, vibration, acoustic emission, cutting temperature and surface roughness [4 - 8]. However, few reliable indirect methods have yet been established for industrial use, mainly because of uncertainty in the correlations between the process parameters and tool wear.

Among the methods given above, the optical methods, even though they stand on an experimental stage in the laboratory, are now considered most promising. This is for several reasons, the main reason being that the recent rapid developments in optoelectronic technology may be successfully adopted in this special application. In addition, suitably fast image processing is being made possible with the advent of appropriate computer hardware. With this motivation, an optoelectronic strategy based on image processing has been developed and tested in this work.

2. Flank wear and tool life criteria

In general, two types of wear apply to tool life, *i.e.* flank wear and crater wear. Flank wear remains the more common measure of tool wear compared with crater wear because of simplicity and ease of measurement. The typical flank wear profile can be divided into three regions as illustrated in Fig. 1: zone C, a nose groove, also known as a trailing groove, which forms near the end of the relief face and contributes significantly to surface roughness; zone N, a leading edge groove which marks the outer end of the wear land, resulting from the rubbing action of the flank face on the uncut diameter of the work, it is generally considered harmless except when it increases the amount of regrinding time and weakens the cutting zone; zone B, a plateau, a more or less uniform wear land, falling between the two grooves.

Two tool life criteria, recommended by the International Standard Organisation, are widely accepted in industry [9, 10]. These criteria are

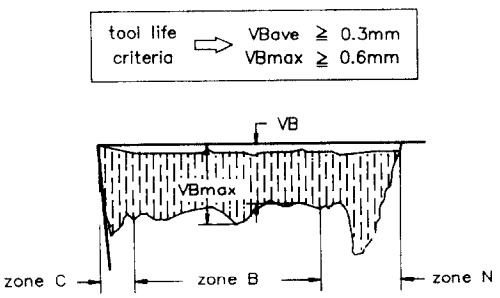

Fig. 1. Typical profile of flank wear and tool wear criteria.

entirely concerned with the profile of the leading edge groove in zone B. If the profile is uniform, the average value VB of the wear land length is measured and a tool can be used unless VB > 0.3 mm. Otherwise, *i.e.* in the case of uneven wear, the maximum peak land length of the groove VB_{max} is taken as the tool life criterion and its limit is 0.6 mm. These two criteria can be summarized as shown below

$$\begin{aligned} &VB \leqslant 0.3 \text{ mm} \\ &VB_{max} \leqslant 0.6 \text{ mm} \end{aligned} \tag{1}$$

It becomes apparent that the entire image of zone B should be examined, so that the average and maximum values of eqn. (1) can be evaluated at the same time.

3. Design of optical measurement system

The experimental apparatus built in this work is shown in Fig. 2 along with a schematic diagram. The system comprises a HeNe laser generator, an object lens (X10), a 0.66 in Vidicon camera, a digital image processing unit and a graphic monitor.

A collimated beam is projected from the laser generator onto the tool tip. The tool is positioned accurately so that its flank face is parallel with the beam in the manner illustrated in Fig. 3. Making the most of its good directionality and brightness, a laser beam is utilized for illumination. The diameter of the beam is 0.8 mm and its full divergence angle lies within 1.0 mrad. The beam used is a 4 mW HeNe laser whose relative intensity is so great that any disturbances from environmental lighting in the workshop can be ignored. It then becomes apparent that no light is reflected from the flank face except from the worn section. Thus if the tool is observed using the Vidicon camera, which is located perpendicular to the flank face, only the view of the flank wear land is observed as no other part is illuminated. The object lens magnifies the view to obtain greater image resolution.

The image of flank wear is formed on the photolayer plate of the Vidicon camera, from which an 8 MHz video signal is produced by the electron beam scanning process. The video signal is then synchronized and converted to a series of 6 bit grey level digital "pixel" data by the image processing unit. An INTEL 8088 CPU supervises all the data acquisition and subsequent image processing procedures. The image frame is made up of 635 X 275 pixels. The image resolution between two consecutive pixels is 0.001 mm.

4. Image processing algorithm

The image processing procedures in this work may be described more readily by introducing mathematical notation in the form of matrix manipu-

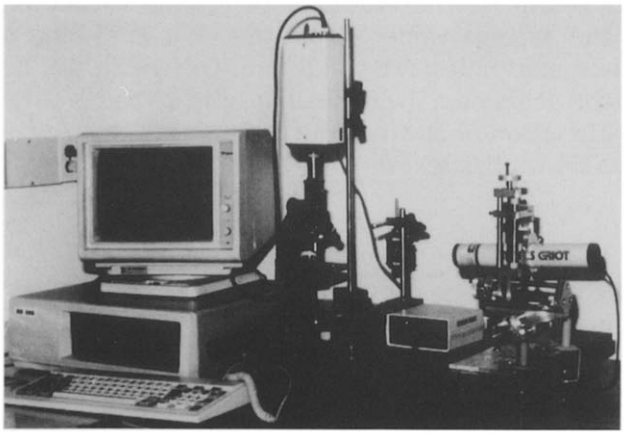

(a)

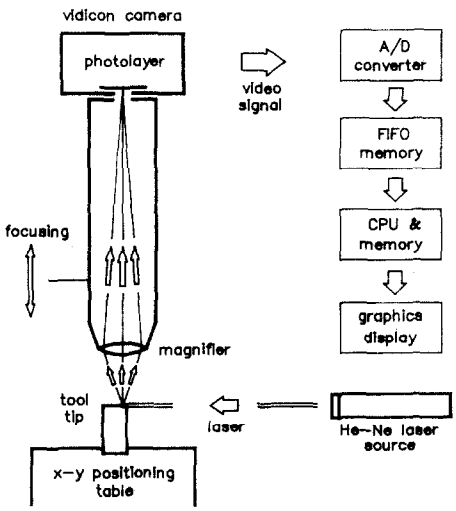

(b)

Fig. 2. Apparatus for tool wear monitoring system. (a) Overall view of apparatus. (b) Schematic diagram of measuring system.

lation. As shown in Fig. 4, an image frame is made up of a two-dimensional array of 635 × 275 pixels. Each pixel is assigned by a position vector $x(i, j)$ in which i indicates the horizontal location and j the vertical location. The origin $x(0, 0)$ is located at the left-upper corner of the image frame. Then, two array variables are defined as

$$I(i, j) \qquad P(i, j)$$
$$i = 0, 1, \ldots, 634 \tag{2}$$
$$j = 0, 1, \ldots, 274$$

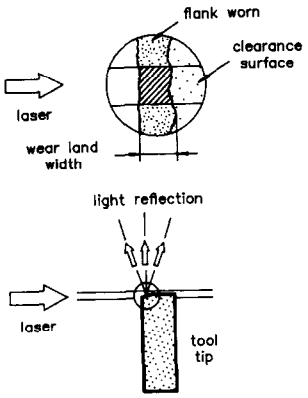

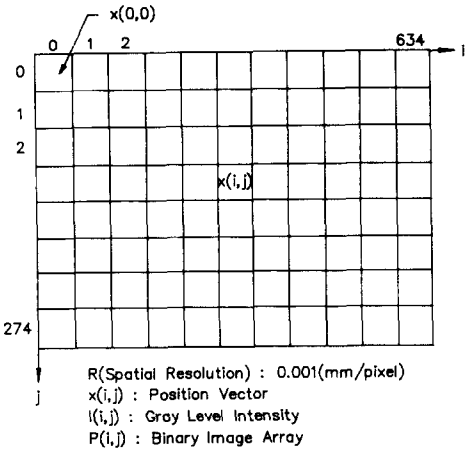

Fig. 3. Illumination of tool tip using laser.

Fig. 4. Mathematical notation of pixel data for image processing.

$I(i, j)$ represents the grey level intensities of the pixels sampled by the Vidicon camera. $P(i, j)$ is the binary image array generated as a result of the image processing.

4.1. Step 1: thresholding

The first step of image processing is thresholding [11]

$$\begin{aligned} P(i,j) &= 1 \quad \text{if } I(i,j) \geqslant I^* \\ P(i,j) &= 0 \quad \text{otherwise} \end{aligned} \tag{3}$$

The threshold limit I^* is defined as a certain level of intensity which gives the clearest image, eliminating noise caused by environmental lighting ang electrical disturbances. The result of this processing is a binary image of $P(i, j)$ as illustrated in Fig. 5. If the whole set of the pixels within the image is denoted by X, it can be divided into subsets as

$$\begin{aligned} \mathrm{X} &= \mathrm{St} \cup \mathrm{Sb} \\ &= (\mathrm{St_h} \cup \mathrm{St_\ell}) \cup (\mathrm{Sb_h} \cup \mathrm{Sb_\ell}) \end{aligned} \tag{4}$$

St represents the pixels within the wear zone surrounded by two border lines and it is supposed to be made up of only high state (or 1) pixels. Alternatively, Sb denotes the background pixels outside the wear zone. In the actual binary image attained by the thresholding process, St is, however, composed of the normal high state subset $\mathrm{St_h}$ and the abnormal low state (or 0) subset $\mathrm{St_\ell}$. $\mathrm{St_\ell}$ is caused by surface irregularities with negative slopes under laser beam illumination, thus no light reflection occurs. In a similar manner, Sb is also affected by features on the flank surface, such as metal chips or surface irregularities. Then, Sb is composed of the normal low state $\mathrm{Sb_\ell}$ and the abnormal high state $\mathrm{Sb_h}$.

4.2. Step 2: noise removal by projection histogram

The noise on the flank surface Sb_h is restored to the low state in this step. The binary data $P(i, j)$ is projected and added along the j axis as

$$f(i) = \sum_{j=0}^{274} P(i, j) \tag{5}$$

Then $f(i)$ constitutes a histogram showing the population of the high state pixels in the j direction. The levels of population provoked by Sb_h are found to be relatively low compared with those provoked by St_h. Thus Sb_h can be removed if $P(i, j)$ is reconfigured as

$$\begin{aligned} &P(i, j) = 0 \quad \text{if } f(i) \leqslant f^* \\ &P(i, j) = P(i, j) \quad \text{otherwise} \end{aligned} \tag{6}$$

in which f^* is the cut-off limit determined by the maximum level of population caused by Sb_h.

4.3. Step 3: contour detection

The wear zone is surrounded by two border lines as depicted in Fig. 5. The border lines can be expressed by defining two variables $Xl(j)$ and $Xr(j)$ for the tool edge line and the wear land line respectively

$$\begin{aligned} &Xl(j) = \min\ [i] \text{ satisfying } C(i, j) = 1 \text{ for each } j \\ &Xr(j) = \max\ [i] \text{ satisfying } C(i, j) = 1 \text{ for each } j \end{aligned} \tag{7}$$

in which

$$\begin{aligned} &C(i, j) = 1 \quad \text{if } \sum_{\substack{\ell=0 \\ m=0}}^{1} P(i + \ell, j + m) \geqslant 3 \\ &C(i, j) = 0 \quad \text{otherwise} \end{aligned} \tag{8}$$

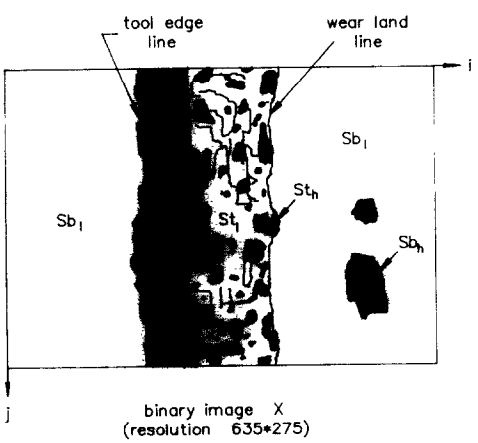

Fig. 5. Map of binary image obtained by thresholding process.

The condition C is set high, *i.e.* the pixel of $x(i, j)$ position vector belongs to the wear zone St if at least three among four neighbouring pixels, including itself, are high. Otherwise, it is set to zero.

4.4. Step 4: contour smoothing

The border lines determined by eqn. (7) are mostly contaminated by undesirable noise St_ℓ. They are therefore recovered by adopting the moving average technique

$$Yl(j) = \sum_{\ell=1}^{(n-1)/2} H_\ell \{Xl(j+\ell) + Xl(j-\ell)\} + H_0 Xl(j) \tag{9}$$

$$Yr(j) = \sum_{\ell=1}^{(n-1)/2} H_\ell \{Xr(j+\ell) + Xr(j-\ell)\} + H_0 Xr(j) \tag{10}$$

where

$j = 0, 1, 2, \ldots, 274$

$H_\ell = 1 - 0.1|\ell|, H_{10} = 0.05$ weighting factor

$H_0 = 1$ weighting factor

$n = 21$

The two new variables $Yl(j)$ and $Yr(j)$ define the smoothed contour of two border lines which are generally more close to actual ones. Then, in order to restore St_ℓ to the high states, $P(i, j)$ can be reconfigured as

$$\begin{aligned} &P(i, j) = 1 \quad \text{if } Yl(j) \leqslant i \leqslant Yr(j) \text{ for each } j \\ &P(i, j) = 0 \quad \text{otherwise} \end{aligned} \tag{11}$$

4.5. Step 5: determination of wear land width

The average value of the wear land width is determined by

$$VB = \frac{R}{275} \sum_{j=0}^{274} \{Yr(j) - Yl(j)\} \tag{12}$$

where R is the image resolution of the two consecutive pixels and the maximum peak land width is taken as

$$VB_{max} = \max\{Yr(j) - Yl(j)\} R \tag{13}$$

5. Results and discussion

A series of measurements were made for various insert-type cutting tools. The results can be well demonstrated on two exemplary tool tips in different states of wear. Figure 6(a) shows their original views using a microscope. Hereafter, they are referred to as specimen 1 and 2.

Figure 6(b) illustrates the consequences of the thresholding process. The resulting images are found to be disturbed by two noise factors: one is the surface irregularities in the wear zone with negative slopes under laser beam illumination, they cause some of the pixels in the subset St to appear in the low state St_{ϱ}; the other factor is the undesirable light scattering elements on the flank face, such as metal chips melted on the tool surface,

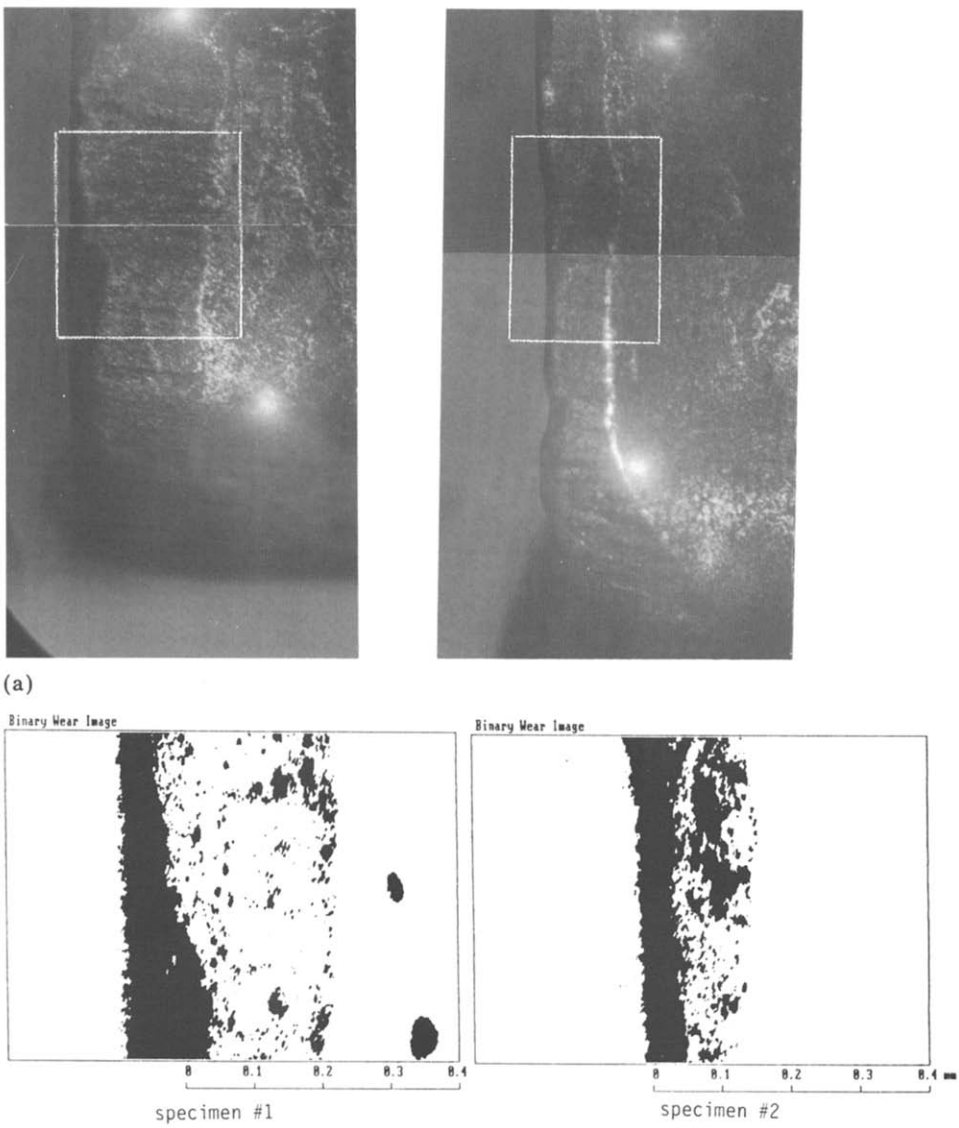

Fig. 6. Original views and binary images of two representative specimens. (a) Original views of specimens taken with a microscope. (b) Binary images of specimens after thresholding process.

Sb_h. This noise generates islands of high state pixels in the subset Sb, as clearly shown on specimen 1 in Fig. 6(b).

The undesirable disturbances on the flank surface Sb_h are removed by the noise removal process using the projection histogram as shown in Fig. 7(a). The cut-off limit f^* was taken as 27, which is 10% of the full popula-

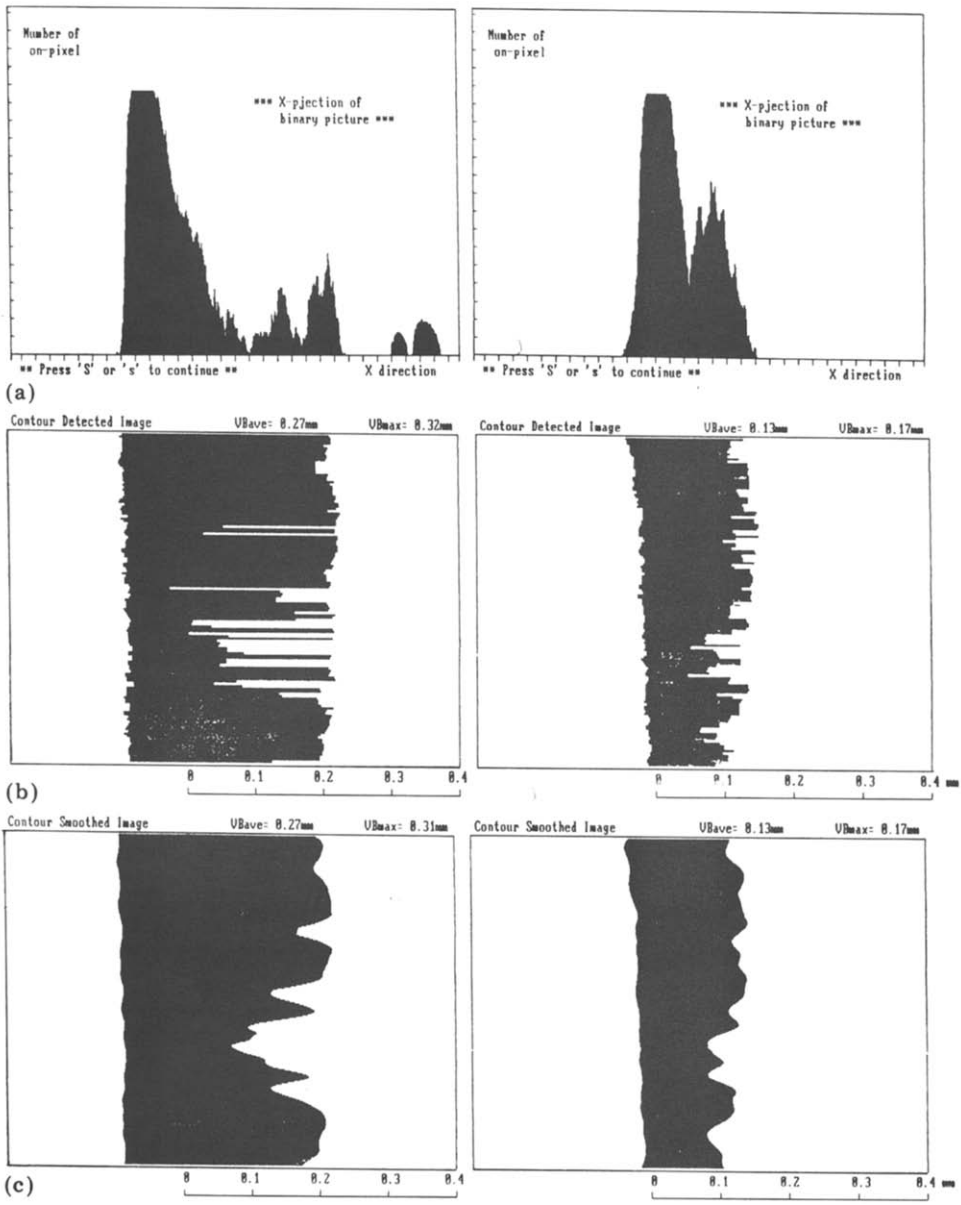

Fig. 7. Binary images of two representative specimens during image processing. (a) *j* projection histograms for noise removal. (b) Binary images after contour detection process. (c) Final binary images after contour smoothing process.

tion in the j axis projection. The binary image in which the noise Sb_h is removed is shown in Fig. 7(b). The tool wear border lines identified in this step are found to fluctuate significantly owing to the noise St_ℓ, especially on specimen 1. The border lines can be smoothed so that their shapes approach the actual wear land lines by adopting the moving average technique. Figure 7(c) shows the final binary images for the two specimens.

The average and maximum peak values of the wear land length were determined using eqns. (12) and (13) as 0.27 mm and 0.31 mm for specimen 1 and as 0.13 mm and 0.17 mm for specimen 2 respectively. The average measuring time for image processing was 1.7 s. The measuring accuracy was found to lie within 0.1 mm when compared with the results obtained using a traditional optical tool microscope.

6. Conclusion

A measurement method for the flank wear of cutting tools has been described. The method is based on real time vision technology and monitors the average and maximum peak values of the wear land width. A prototype measuring system was built and tested using the image processing algorithm specially developed for *in situ* applications. Experimental results showed that the method was very effective, being capable of detecting tool wear to an accuracy of 0.1 mm within 1.7 s processing time.

This measuring method may be adopted for CNC lathes for automatic inter-process monitoring of tool wear as shown in Fig. 8. The optical and electronic hardware can be miniaturized and attached to the machine as a tool wear inspection station. The tool can then be positioned accurately by numerical control for the optical measurement developed in this work. Information on tool wear can be supplied to the CNC controller in the form of digital data, thus tool wear compensation can be accomplished if any reliable adaptive control algorithm is available.

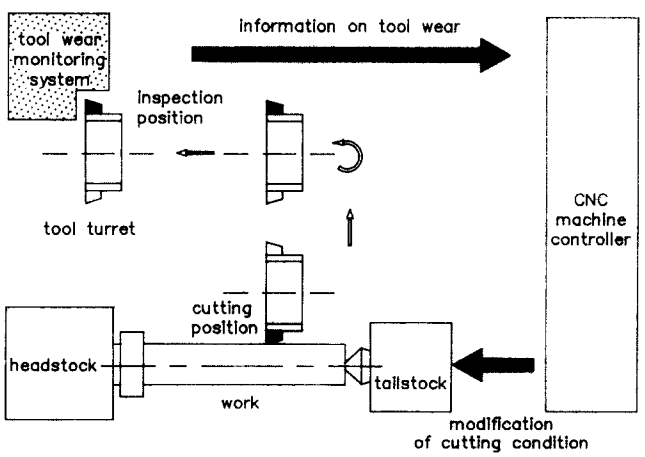

Fig. 8. Possible configuration for tool wear control.

References

1 G. F. Micheletti and W. Koenig, In-process tool wear sensors for cutting operations, *Ann. CIRP, 25* (2) (1976) 483 - 496.

2 E. H. Frost-Smith *et al.*, Optimization of the machining process and overall system concepts, *Proc. MTIRA Conf. on Adaptive Control of Machine Tools, April, 1970.*

3 K. Yamazaki, A. Yamada, S. Sawai and H. Takeyama, A study on adaptive control in an NC milling machine, *Ann. CIRP, 23* (1) (1974) 153 - 154.

4 K. Taraman, R. Swando and W. Yamauchi, Relationship between tool forces and flank wear, *SME Tech. Paper MR74/704*, 1974.

5 M. C. Shaw and S. R. Shangbani, On the origin of cutting vibrations, *CIRP General Assembly, 1962.*

6 K. Iwata and T. Moriwaki, An application of acoustic emission measurement to in-process sensing of tool wear, *Ann. CIRP, 26* (1) (1977) 21 - 26.

7 F. Giusti and M. Santochi, A flexible tool wear sensor for NC lathes, *Ann. CIRP, 33* (1) (1984) 229 - 232.

8 K. Uehara, New attempts for short time tool-life test, *Ann. CIRP, 22* (1) (1973) 23 - 24.

9 G. Boothroyd, *Fundamentals of Metal Machining and Machine Tools*, McGraw-Hill, New York, 1975.

10 V. C. Venkatesh and M. Satchithanandam, A discussion on tool life criteria and total failure causes, *Ann. CIRP, 29* (1) (1980) 19 - 22.

11 J. S. Weszka, R. N. Nagel and A. Rosenfeld, A threshold selection technique, *IEEE Trans. Comput., C-23* (1974) 1322 - 1326.